Journal of Applied Biomechanics, 2012, 28, 387-393

Journal of
APPLIED BIOMECHANICS
An Official Journal of ISB
www.JAB-Journal.com
ORIGINAL RESEARCH

Influence of Shear Stress on Behaviors of Piezoelectric Voltages in Bone

Donghui Fu,[1] Zhende Hou,[1] Qing-Hua Qin,[2] Lianyun Xu,[1] and Yanjun Zeng[3]
[1]Tianjin University; [2]Australian National University; [3]Beijing University of Technology

The piezoelectric properties of bone play an important role in the bone remodeling process and can be employed in clinical bone repair. In this study, the piezo-voltage of bone between two surfaces of a bone beam under bending deformation was measured using an ultra-high-input impedance bioamplifier. The influence of shear stress on the signs of piezo-voltages in bone was determined by comparing and contrasting the results from three-point and four-point bending experiments. From the three-point bending experiment, the study found that the signs of piezo-voltages depend only on shear stress and are not sensitive to the normal stress.

Keywords: piezoelectricity, collagen, composite

The piezoelectric properties of bone were discovered in the 1950s (Fukada & Yasuda, 1957). They were reported to have an effect on the bone remodeling process (Fukada & Yasuda, 1957; Bassett & Becker, 1962; Steinberg et al., 1968; Qin & Ye, 2004; Qin et al., 2005). It was thought that the potentials in bone generated by stress are likely to have an impact on bone remodeling. In the literature, the piezoelectric behavior of bone was thought to be similar to that in mineral piezoelectric materials and to belong to Point group C6 or D6 (Fukada, 1964; Aschero et al., 1999; Otter et al., 1985). Since then, many studies have focused on determining the piezoelectric coefficients of bone and the piezoelectric equations (Fukada, 1964; Marino & Gross, 1989; Korostoff, 1977; Guzelsu, 1978). However, bone has a complex hierarchical structure and its piezoelectric properties may vary from point to point, which means that there is no uniform piezoelectric coefficient matrix in bone tissues (Fukada, 1964; Marino & Gross, 1989; Korostoff, 1977). The complexities of bone piezoelectricity have led to the development of various methods to investigate the piezoelectric properties of bone. For example, based on the converse piezoelectric effect of bone, the piezoelectric coefficient d_{23} was determined by using a sensitive dilatometer (Aschero et al., 1999). A piezoelectric force microscope and an atomic force microscope have also been employed to measure the piezoelectric properties of bone or collagen of bone (Kalinin et al., 2005; Minary-Jolandan & Yu, 2009; Halperin et al., 2004).

In recent years, various artificial biomaterials have been developed and used as bone substitutes that have biocompatibility and bioactivity, and are osteoconductive. Those materials are implanted in living body for repairing bone defects and recovering normal bone function. Since substitutes with piezoelectric properties can stimulate osteocyte growth and bone formation in vivo (Baxter et al., 2008; Silva et al., 2001; Miara et al., 2005), it can be concluded that the surface potential of both the substitutes and bone or their combinations have stimulatory effects on osteocyte growth. This explains the clinical significance and motivation for the research into the piezoelectric behavior of bone.

Piezoelectric signals from bone have been obtained mainly by measuring electric charges or deformations induced due to the converse piezoelectric effect (Fukada & Yasuda, 1957; Aschero et al., 1999) because measuring piezoelectric charges is relatively easier technically than measuring piezoelectric voltages. However, the piezoelectric voltage can directly reflect the electric environment of bone surfaces. That is the motivation for developing experimental approaches to measure piezoelectric voltage. In this study, the piezo-voltage of bone under bending deformation was measured using an ultra-high-input impedance bioamplifier. The influence of shear stress on the behavior of piezo-voltage in bone was evaluated by comparing and contrasting the results from three-point and four-point bending experiments. The study demonstrates theoretically from the three point bending experiment that no matter how small the shear stress is and how large the normal stress is, the signs of piezo-voltages depend only on shear stress.

Donghui Fu, Zhende Hou *(Corresponding Author)*, and Lianyun Xu are with the Department of Mechanics, School of Mechanical Engineering, Tianjin University, Tianjin, China. Qing-Hua Qin is with the Research School of Engineering, Australian National University, Canberra, ACT, Australia. Yanjun Zeng is with the Biomechanics & Medical Information Institute, Beijing University of Technology, Beijing, China.

Methods

In the experiment, cortical bone materials were harvested from the mid-diaphysis of dry bovine (age 2–3 years) tibias, and machined into beam samples with their axis aligned with the longitudinal direction of the diaphysis (Figure 1(a)). Ten samples were prepared with the dimension range as illustrated in Table 1. Conductive silver adhesive (5001, SPI, USA) was painted on both sides of the specimens as electrodes with dimensions of 3 mm × 3 mm. There were two types of specimen with different electrode distribution. Figure 1(b) shows type A with six pairs of electrodes and Figure 1(c) shows type B with two pairs of electrodes. Two electrodes on both lateral sides of a sample comprised a pair of electrodes located at the same height of both lateral sides as shown in Figure 1. The electrodes attached to the type A sample are denoted by the numbers 1 through 6 on one side and 1′ through 6′ for the corresponding electrodes on the other side, facing the medullary cavity. Then 1–1′ to 6–6′ represent the six pairs of electrodes respectively, and similarly 7–7′ to 8–8′ represent the two pairs of electrodes on the type B sample. When the samples were subjected to four-point bending, all of the six pairs of electrodes on type A samples experienced pure bending deformation, whereas on Type B samples, only electrodes 8–8′ experienced pure bending deformation.

The experimental setup of the measurement system used is illustrated in Figure 2. Taking as reference an electrode on the lateral side facing the medullary cavity, such as 3′, the measured piezo-voltage between the pair of electrodes 3–3′ was input into a bioamplifier (BMA-931, CWE Inc., USA) via an ultra-high-input impedance (over 10^{12} Ω) head stage (Super Z, CWE Inc., USA). The amplified voltage signals were then recorded by a computer in the measurement system. Mechanical loadings were applied using an Instron 1343 closed-loop servo-hydraulic machine controlled by an 8800 control tower, and the loading signals in the control tower were also input into the computer for recording.

The testing sample and the head stage were enclosed in a double electromagnetic shield with the outer shield connecting to earth and the inner to the head stage common terminal. This arrangement kept the electric field constant around the sample (Fu et al., 2006; Hou et al., 2011).

A trapezoidal loading profile was used, with a loading (or unloading) rate of 600 N·s^{-1}, load holding time of 6 s, and a holding load of 300 N, which produced maximum tensile (or compressive) stresses from 24 to 45 MPa in the samples, being well below the tensile strengths of 50–100 MPa of cortical bovine bone (Cowin, 1983). The trapezoidal loading waveform is shown in Figure 3(a). Figure 3(b) shows a typical piezo-voltage waveform between electrodes 3–3′ under three-point bending. The waveform has two pulses with different signs, corresponding to the loading and unloading processes respectively. The peak of the first pulse corresponds to the loading endpoint and the second pulse peak corresponds to the unloading endpoint. This shows that once the loading or unloading process ends the corresponding piezo-voltage began to decrease toward zero. In other words, the polarized charges or piezo-voltages appeared on the bone surfaces in pulse form as the bone deformation varied with loading (Fu et al., 2006; Hou et al., 2011).

Table 1 Dimension range of samples

Span (mm)	Width (mm)	Height (mm)
85	4.0 ± 1.0	19 ± 3.0

Results

Figure 4 shows a group of typical results of a type A sample. Figure 4(a)–(e) corresponds to the arrangement of electrodes on bone samples. There are two plots of piezo-voltage vs. time in each figure. The black plot represents the result from the three-point bending test and the red represents the result from the four-point bending test.

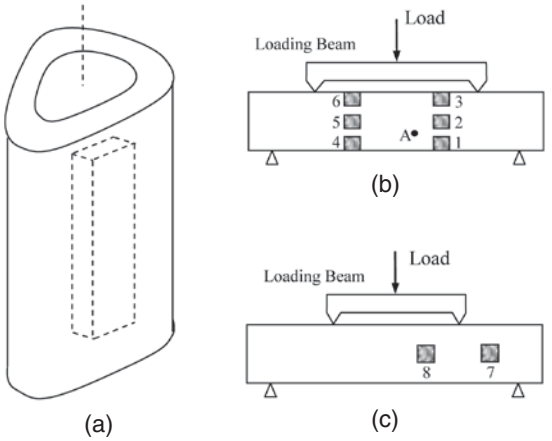

Figure 1 — Sample and electrode arrangements.

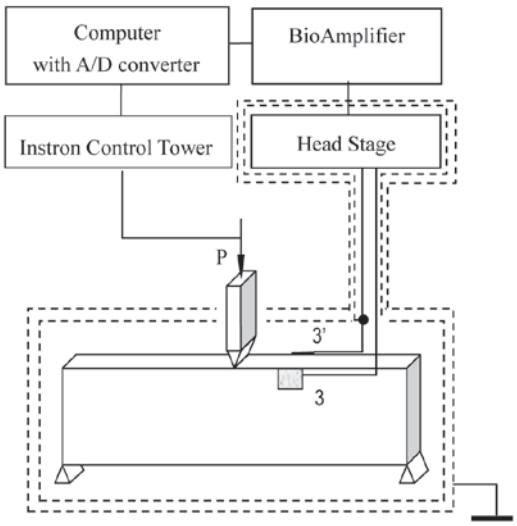

Figure 2 — Setup of the test system.

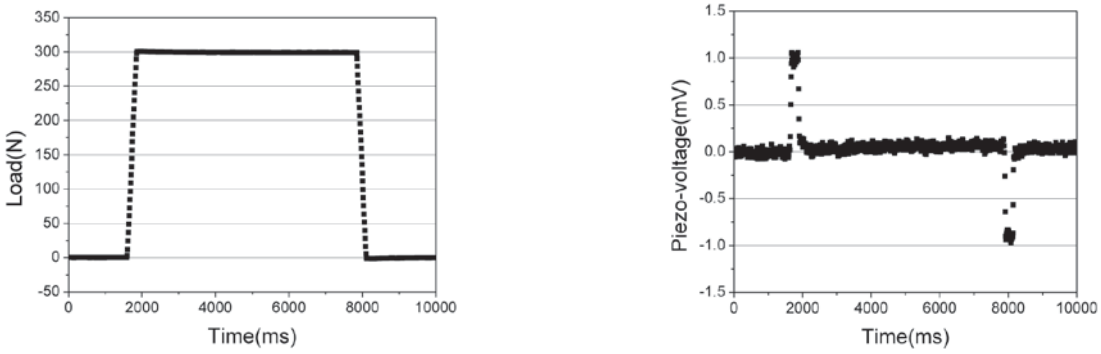

(a) Loading waveform (b) Piezo-voltage waveform

Figure 3 — Loading and piezo-voltage wave form. (a) Loading waveform. (b) Piezo-voltage waveform.

All five type A samples show similar plots of piezo-voltage vs. time under three-point bending. However, in the plots from the four-point bending, the shapes are similar but the signs are opposite. Table 2 shows all the voltage peak values of the sample type A plots, under three- and four-point bending tests.

Figure 5 shows the results of piezo-voltage vs. time for type B samples under the loading profile shown in Figure 3. It can be seen from Figure 5 that the signs of the piezo-voltage are the same as those shown in Figure 4. Table 3 lists all the peak values of piezo-voltage for the type B samples.

Discussion

The results in the preceding section indicate that in the case of three-point bending, the signs of the piezo-voltage at electrodes 1–1′ through 3–3′ were opposite to those at electrodes 4–4′ through 6–6′, and those at electrodes 7–7′ and 8–8′ of the type B sample had the same sign as those at electrodes 1–1′ through 3–3′ of the type A samples. In the case of four-point bending, the piezo-voltages of all the electrodes of the type A samples and electrode 8–8′ of the type B sample were lower than those obtained from the three-point bending test. Moreover, the piezo-voltages of the electrodes near the neutral axis in the pure bending zone, such as 2–2′, 5–5′, and 8–8′, were approximately zero. Nevertheless, the piezo-voltage signs of electrodes 1–1′, 3–3′, 4–4′ and 6–6′, which were little distant from the neutral axis, were random or irregular. In contrast, the sign and peak of the piezo-voltage of electrode 7–7′, which was outside the pure bending zone, were similar to those under three-point bending test.

The analysis and observations can be summarized as follows: (1) The differences in the piezo-voltage signs between the two groups of electrodes 1–1′ through 3–3′ and 4–4′ through 6–6′ are due to the fact that normal stress is distributed symmetrically and shear stress is distributed antisymmetrically about the loading axis in the sample under three-point bending. This means that the signs of piezo-voltage depend on shear stress only. It should be mentioned that the signs of the piezo-voltage at electrodes 7–7′ and 8–8′ being the same as those at electrodes 1–1′ through 3–3′ under three-point bending also supports that conclusion because electrodes 7–7′ and 8–8′ are located around the neural axes and only shear stresses act around them. (2) For both types of sample there is only normal stress in any cross-section in the pure bending zone. Within the pure bending zone, the piezo-voltages at all the electrodes become lower, but they do not approach zero except for electrodes 2–2′, 5–5′, and 8–8′, which are located around the neutral axes. It can be concluded that the peak values of the piezo-voltages depend mainly on shear stress although normal stress still contributes to some extent. (3) As can be seen from Tables 2 and 3, the peak values at the same electrodes in different samples are relatively irregular. These irregularities occur either between samples or between electrodes. This indicates that the piezoelectricity of bone depends on the hierarchical structure of bone, which might differ in different samples. The important conclusion as to the macroscopic piezoelectric property of bone, however, is that the signs of piezo-voltages between two lateral surfaces depend on shear stress only, not on normal stress.

It is noted from the analysis above that irregularities in the piezo-voltage results suggest that the piezoelectric properties of bone are relevant to its microstructure. Cortical bone has been regarded as a hierarchical composite material comprised of mineral and organic phases. The mineral phase is mainly composed of crystalline hydroxyapatite and the organic phase consists mainly of collagen, which is the origin of piezoelectricity (Steinberg et al., 1968; Fukada, 1964; Minary-Jolandan & Yu, 2009).

Figure 6 shows a schematic illustration of collagen fibers (Jager & Fratzl, 2000; Fratzl & Weinkamer, 2007). A collagen molecule is about 300 nm in length and about 1.5 nm in diameter. There is a 40 nm gap between the ends of collagen molecules in the longitudinal direction, and 27 nm of a 300 nm collagen molecule length overlaps with the adjacent collagen molecule. There is a covalent cross-link in the overlap region connecting adjacent collagen molecules. Collagen molecules are filled and coated by platelet-like tiny mineral crystals, which form

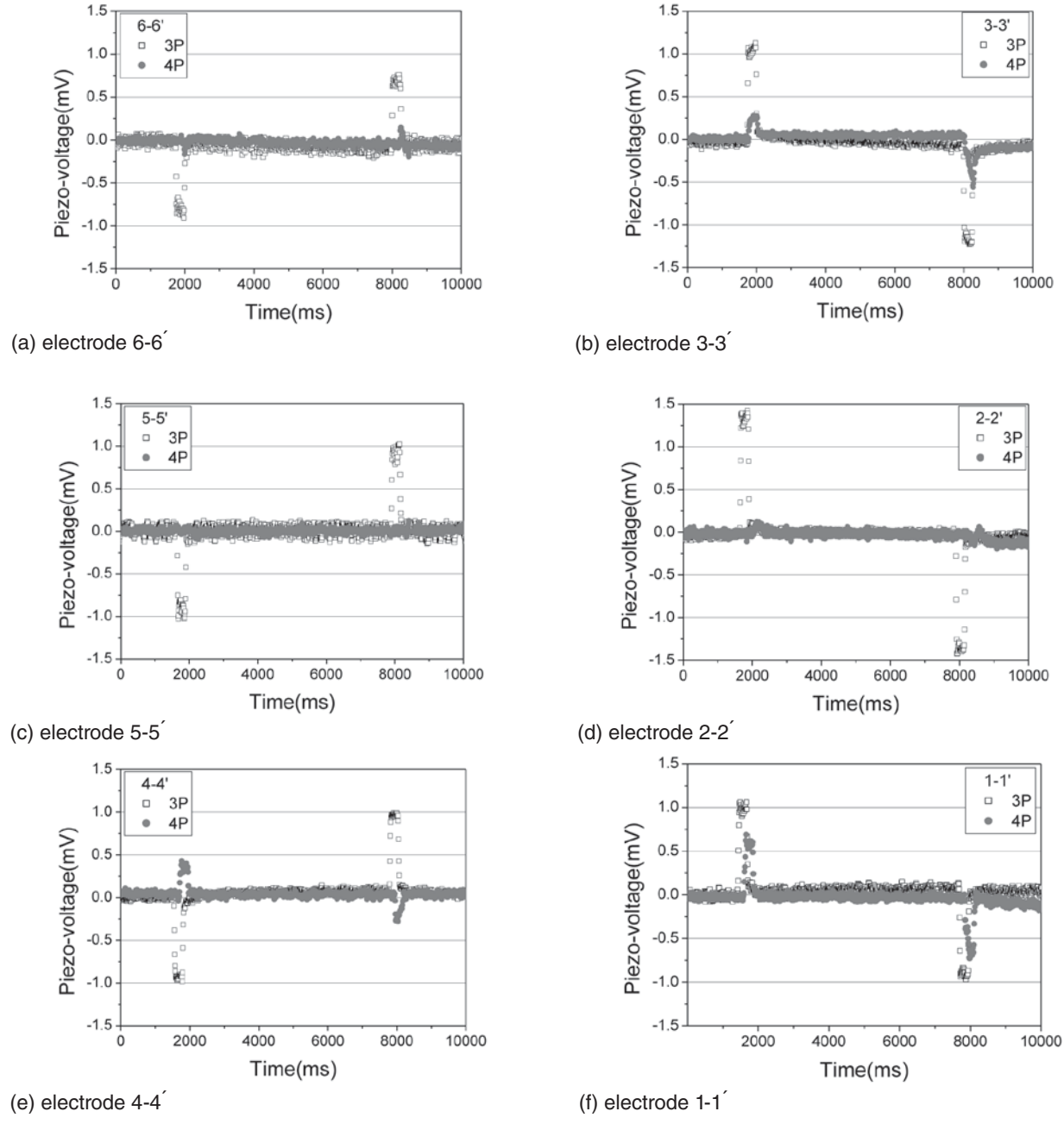

Figure 4 — Typical plots of piezo-voltage vs. time for type A sample.

the mineralized collagen fibril. A group of collagen fibrils embedded with the mineral crystals forms the hierarchical structure of collagen fiber.

Let the square area in Figure 6 represent a segment of mineral collagen. A theoretical model representing the segment is employed in this section (Wang & Qian, 2006). The model has a collagen layer sandwiched between two mineral layers (Figure 7a). Although collagen fibrils are oriented in various directions in bone, they are oriented primarily in the mean direction parallel to the axis of bone diaphysis (Ascenzi & Lomovtsev, 2006; Bills et al., 1982) or the axis of the samples. As a force acting on a collagen fiber in any direction can be divided into normal force and shear force, it can be assumed that the mineral collagen in the model is parallel to the sample axis, without loss of generality. The model can be analyzed using "shear lag" theory (Wang & Qian, 2006; Kotha & Guzelsu, 2000). Based on shear lag theory, it is assumed that the mineral phase carries only normal load and the collagen phase carries only shear load (Figure 7b). The external normal stresses σ_0 and σ_1 can be determined using traditional beam theory. According to the reciprocal theorem of

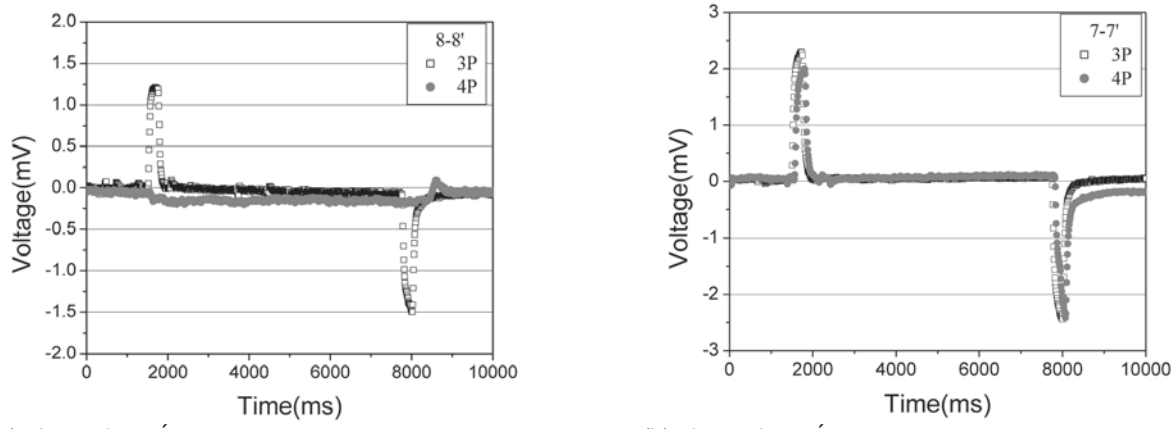

(a) electrode 7-7′ (b) electrode 8-8′

Figure 5 — Typical plots of piezo-voltage vs. time for type B sample.

Table 2 Piezo-voltage peak values (mV) for type A sample under 3- and 4-point bending

Sample type A	Electrodes											
	1–1′		2–2′		3–3′		4–4′		5–5′		6–6′	
	3P	4P	3P	4P	3P	4P	3P	4P	3P	4P	3P	4P
1	1.06	0.69	1.71	0.10	1.23	–0.28	–0.49	0.43	–1.28	–0.10	–0.94	–0.17
2	3.27	0.72	4.33	0.19	1.78	–0.44	–1.92	0.55	–3.94	0	–2.13	–0.31
3	1.35	0.40	1.32	0	1.30	0.56	–1.35	–0.47	–1.66	0.14	–0.77	0
4	0.81	0.54	2.65	0	2.47	0.80	–1.75	–0.42	–1.87	0	–0.79	0.32
5	2.39	0.76	1.10	–0.15	1.63	–0.15	–2.10	–0.22	–0.99	–0.20	–1.57	–0.50

Table 3 Piezo-voltage peak values (mV) for type B sample under 3- and 4-point bending

Sample type B	Electrode 7–7′		Electrode 8–8′	
	3P	4P	3P	4P
1	2.30	1.99	1.20	–0.20
2	1.86	2.03	0.65	0
3	3.07	3.04	1.38	0
4	1.79	1.90	1.76	0.30
5	3.68	3.40	4.01	0.18

shear stress, the shear stresses τ_0 and τ_1 are equal to the corresponding shear stresses on the cross-section. The shear stresses at any point on the cross-section can also be determined by using traditional beam theory.

Let h and w be the widths of the collagen and mineral components respectively, and the model thickness is one unit. The force equilibriums of the isolated elements (Figure 7c) are derived using the analysis method reported in the literature (Wang & Qian, 2006):

$$w\frac{d\sigma_0}{dx} + \tau_0 + \tau = 0 \qquad (a)$$

$$w\frac{d\sigma_1}{dx} - \tau - \tau_1 = 0 \qquad (b)$$

Let u_0 and u_1 be displacements of the two mineral components respectively, and assume the mineral component is linear elastic. Then

$$\sigma_0 = E\frac{du_0}{dx}, \quad \sigma_1 = E\frac{du_1}{dx}, \quad \tau = G\gamma$$

where E is the elastic modulus of the mineral phase, G is the shear elastic modulus, γ is the shear strain in the collagen layer. γ is also equal to

$$\gamma = \frac{u_1 - u_0}{h},$$

Substituting the above three equations into Eqs. (a) and (b), and then subtracting (a) from (b) yields

$$wE_m h\frac{d^2\gamma}{dx^2} - 2G\gamma = \tau_0 + \tau_1 \qquad (c)$$

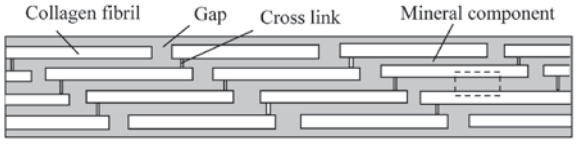

Figure 6 — A schematic illustration of mineral collagen fiber.

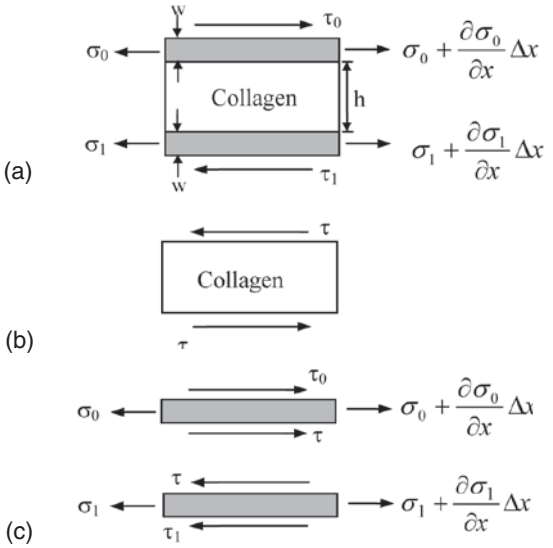

Figure 7 — A schematic presentation of the model.

with the following boundary conditions:

$\gamma|_{x=\infty}$= a bounded value, and also $\gamma|_{x=0}$= a bounded value.

Because the origin is a relative position, it can be considered that $\gamma|_{x=0} = 0$.

Finally, the solution is

$$\gamma(x) = -\frac{\tau_0 + \tau_1}{2G}\left(1 - e^{-\sqrt{\frac{2G}{wE_m h}}x}\right) \qquad (d)$$

Solution (*d*) indicates that the sign of shear strain γ depends entirely on the difference between τ_0 and τ_1 ($\tau_0 > \tau_1$ according to traditional beam theory). The conclusion can be drawn that the shear stress determined by traditional beam theory is responsible for the sign of piezo-voltage in bone. Because the exponent term in Eq. (*d*) includes elastic modulus *E*, normal stresses still contribute to the shear strain. However, the normal stress can only change the amplitudes, not the sign of the shear strain. That is, no matter how small τ_0 and τ_1 are, or how large the normal stresses σ_0 and σ_1 are, the signs of shear strain in collagen fibrils depend exclusively on the shear stresses τ_0 and τ_1. This conclusion explains why the signs of piezo-voltages remain the same with shear stress under three-point bending.

It was demonstrated experimentally and theoretically that the signs of piezo-voltages of bone under bending deformation depend only on shear stress. It seems doubtful that normal stress contributes only to the amplitude of piezo-voltage and not to changing its sign. If normal stress itself can generate a piezo-voltage in bone, it must dominate the sign of the voltage, as a voltage is a physical quantity with both magnitude and sign. A possible reason is the coupling effect between normal stress and shear stress. Macroscopically, only normal stress is operating on a cross-section of a sample under four-point bending. However, because cortical bone has a hierarchical structure and collagen fibrils are distributed in the mineral matrix in a very complex and random manner, the coupling effect between normal stress and shear stress becomes microscopically stronger. Perhaps the piezo-voltages in the pure bending zone of the sample under four-point bending arose from the coupled shear stresses. If so, the contribution of normal stress to piezo-voltages in bone still comes substantially from shear stresses. Other possible contributors to bone piezoelectricity are the cross-links, which are covalent bonds between two adjacent collagen molecules (Figure 6). Pollack et al. (1977) found experimentally that the piezoelectricity of bone increased with an increasing amount of cross-links. Minary-Jolandan and Yu (2009) formed the opinion that the cross-links enable collagen molecules to transmit mechanical forces to neighboring collagen molecules. In terms of their transmission function, the cross-links are affected by shear stress. The contribution of piezo-signals from the cross-links to the piezo-voltages from the bending experiment is an interesting research issue.

Acknowledgments

The work is supported by the National Natural Science Foundation of China under grant No.10672119.

References

Ascenzi, M.G., & Lomovtsev, A. (2006). Collagen orientation patterns in human secondary osteons, quantified in the radial direction by confocal microscopy. *Journal of Structural Biology, 153,* 14–30. PubMed doi:10.1016/j.jsb.2005.08.007

Aschero, G., Gizdulich, P., & Mango, F. (1999). Statistical characterization of piezoelectric coefficient d23 in cow bone. *Journal of Biomechanics, 32,* 573–577. PubMed doi:10.1016/S0021-9290(99)00021-4

Bassett, C.A.L., & Becker, R.O. (1962). Generation of electric potentials by bone in response to mechanical stress. *Science, 137,* 1063–1069. PubMed doi:10.1126/science.137.3535.1063

Baxter, F.R., Turner, I.G., Bowen, C.R., Gittings, J.P., Chaudhuri, J.B., & Lewis, R.W.C. (2008). The Structure and Properties of Electroceramics for Bone Graft Substitution. *Key Engineering Materials, 361-363,* 99–102. doi:10.4028/www.scientific.net/KEM.361-363.99

Bills, P.M., Lewis, D., & Wheeler, E.J. (1982). Mineral-collagen orientation relationships in bone. *Journal of Chemical Crystallography, 12,* 51–63.

Cowin, S.C. (1983). The mechanical and stress adaptive properties of bone. *Annals of Biomedical Engineering, 11,* 263–295. PubMed doi:10.1007/BF02363288

Fratzl, P., & Weinkamer, R. (2007). Nature's hierarchical materials. *Progress in Materials Science, 52,* 1263–1334. doi:10.1016/j.pmatsci.2007.06.001

Fu, D.H., Hou, Z.D., & Qin, Q.H. (2006). Analysis of the waveforms of piezoelectric voltage of bone. *Journal of Tianjin University, 39,* 349–353.

Fukada, E., & Yasuda, I. (1957). On the piezoelectric effect of bone. *Journal of the Physical Society of Japan, 12,* 1158–1162. doi:10.1143/JPSJ.12.1158

Fukada, E. (1964). Piezoelectic effects in collagen. *Japanese Journal of Applied Physics, 3,* 117–121. doi:10.1143/JJAP.3.117

Guzelsu, N. (1978). A piezoelectric model for dry bone tissue. *Journal of Biomechanics, 11,* 257–267. PubMed doi:10.1016/0021-9290(78)90052-0

Halperin, C., Mutchnik, S., Agronin, A., Molotskii, M., Urenski, P., Salai, M., & Rosenman, G. (2004). Piezoelectric Effect in Human Bones Studied in Nanometer Scale. Nano. *Nano Letters, 4,* 1253–1256. doi:10.1021/nl049453i

Hou, Z.D., Fu, D.H., & Qin, Q.H. (2011). An exponential law for stretching- relaxation properties of bone piezovoltages. *International Journal of Solids and Structures, 48*(3-4), 603–610. doi:10.1016/j.ijsolstr.2010.10.024

Jager, I., & Fratzl, P. (2000). Mineralized collagen fibrils: a mechanical model with a staggered arrangement of mineral particles. *Biophysical Journal, 79,* 1737–1746. PubMed doi:10.1016/S0006-3495(00)76426-5

Kalinin, S.V., Rodriguez, B.J., & Jesse, S. (2005). Thundat T, Gruverman A. Electromechanical imaging of biological systems with sub-10 nm Resolution. *Applied Physics Letters, 87,* 053901. doi:10.1063/1.2006984

Korostoff, E. (1977). Stress Generated potentials in bone: relationship to piezoelectricity of collagen. *Journal of Biomechanics, 10,* 41–44. PubMed doi:10.1016/0021-9290(77)90028-8

Kotha, S.P., & Guzelsu, N. (2000). The effects of interphase and bonding on the elastic modulus of bone: changes with age-related osteoporosis. *Medical Engineering & Physics, 22*(8), 575–585. PubMed doi:10.1016/S1350-4533(00)00075-8

Marino, A.A., & Gross, B.D. (1989). Piezoelectricity in cementum, dentine and bone. *Archives of Oral Biology, 34,* 507–509. PubMed doi:10.1016/0003-9969(89)90087-3

Miara, B., Rohan, E., Zidi, M., & Labat, B. (2005). Piezomaterials for bone regeneration design-homogenization approach. *Journal of the Mechanics and Physics of Solids, 53,* 2529–2556. doi:10.1016/j.jmps.2005.05.006

Minary-Jolandan, M., & Yu, M.F. (2009). Uncovering Nanoscale Electromechanical Heterogeneity in the Subfibrillar Structure of Collagen Fibrils Responsible for the Piezoelectricity of Bone. *ACS Nano, 3,* 1859–1863. PubMed doi:10.1021/nn900472n

Otter, M., Shoenung, J., & Williams, W.S. (1985). Evidence for different sources of stress-generated potentials in wet and dry bone. *Journal of Orthopaedic Research, 3,* 321–324. PubMed doi:10.1002/jor.1100030308

Pollack, S.R., Korostoff, E., Sternberg, M.E., & Koh, J. (1977). Stress-Generated potentials in bone: effects of collagen modifications. *Journal of Biomedical Materials Research, 11*(5), 677–700. PubMed doi:10.1002/jbm.820110505

Qin, Q.H., & Ye, J.Q. (2004). Thermolectroelastic solutions for internal bone remodeling under axial and transverse loads. *International Journal of Solids and Structures, 41*(9-10), 2447–2460. doi:10.1016/j.ijsolstr.2003.12.026

Qin, Q.H., Qu, C.Y., & Ye, J.Q. (2005). Thermolectroelastic solutions for surface bone remodeling under axial and transverse loads. *Biomaterials, 26*(33), 6798–6810. PubMed doi:10.1016/j.biomaterials.2005.03.042

Silva, C.C., Lima, C.G.A., Pinheiro, A.G., Goes, J.C., Figueiro, S.D., & Sombra, A.S.B. (2001). On the piezoelectricity of collagen.chitosan films. *Physical Chemistry Chemical Physics, 3,* 4154–4157. doi:10.1039/b100189m

Steinberg, M.E., Bosch, A., Schwan, A., & Glazer, R. (1968). Electrical potentials in stressed bone. *Clinical Orthopaedics and Related Research, 61,* 294–300. PubMed doi:10.1097/00003086-196811000-00033

Wang, X., & Qian, C. (2006). Prediction of microdamage formation using a mineral-collagen composite model of bone. *Journal of Biomechanics, 39,* 595–602. PubMed doi:10.1016/j.jbiomech.2005.01.009